2018 26th Mediterranean Conference on Control and Automation (MED)
Zadar, Croatia, June 19-22, 2018

A pHRI framework for modifying a robot's kinematic behaviour via varying stiffness and dynamical system synchronization.

Theodora Kastritsi[1], Antonis Sidiropoulos[1] and Zoe Doulgeri[1]

Abstract— **In this work, we propose a robot control framework for modifying a desired robot kinematic behavior encoded in dynamical movement primitives (DMP) by physically interacting with the robot during its autonomous operation. The proposed method is based on variable stiffness and DMP time synchronization with the user during the interaction. The overall controlled system is proved to be stable. After the user stops interacting with the robot, the robot motion continues according to the learned kinematic behavior until it reaches the final task goal. At the next execution cycle a new DMP can been learned to generate the modified trajectory. In this way, explicit robot programming and separation of learning and execution stages is eliminated. The proposed approach is implemented and evaluated on a 7-degree-of-freedom KUKA LWR4.**

I. INTRODUCTION

As robotics move away from their traditional use behind fences and into a more dynamic and uncertain environments, motion planning is abandoned in favor of kinematic behavior models utilizing dynamical systems (DS). DS act as motion generators, producing a motion reference by solving a differential equation on-line, thus being robust to target changes. They usually encode rich kinematic behaviors that are learned by demonstration. A simple way to demonstrate a kinematic behavior is by utilizing physical human robot interaction (pHRI) as kinesthetic teaching. The most popular form of DS is the Dynamic Movement Primitives (DMP), which was introduced by Schaal et.al [1] having a unique attractor at the target. The DMP framework allows spatial and temporal scaling as well as online coupling terms inducing phase stopping, to stop the time evolution in case a disturbance acts on the robot, or modifications that force the DMP state to remain close to the perturbed robot [2]. Nevertheless, one can distinguish two distinctive steps in the above methods, one for the demonstration and one for the autonomous execution of the learned trajectory. In this work we are interested in unifying the two steps into one in order to allow modifications of the learned motion via pHRI while the robot executes the learned DMP; hence we consider the external human force as a voluntary intervention rather than a disturbance. Our aim raises the issues of the robot's compliance and the DMP's motion synchronization with the human's intervention so that motion modifications are enabled in parallel with DMP execution. A first attempt to approach the parallel use of DMP motion generation with human interventions is proposed in the progressive automation framework of [3] without motion synchronization and stability considerations. To our knowledge, attempts of motion synchronization have been reported only in the case of rhythmic movements via the adaptation of the motion's angular frequency [4].

Several works propose a variable impedance strategy to control a robot while interacting with humans. Most of them focus on kinesthetic guidance thus setting target stiffness to zero while adapting the damping and mass parameters based on the human's velocity [5], both the velocity and acceleration [6] and/or the time derivative of the force [7]. In surgical or industrial applications variable stiffness is employed to ensure the tracking accuracy of a desired trajectory as well as stiffness adaptation during physical interaction with the user or the environment. Stability of a robotic system with a variable target stiffness has been addressed in few works; in [8] the utilization of the tank energy approach is proposed to resolve the passivity loss induced by the variable stiffness. In the tank-based approach, initially introduced in [9], the dissipated energy of the robotic system is added to a virtual tank from which it can be extracted in order to implement stiffness variations.

In this work we propose a control method for a robot under varying stiffness whose motion is generated by a DMP novel structure allowing synchronization with the user. When the user intervenes, stiffness is adapted and the DMP's time evolution is synchronized facilitating and accommodating any trajectory modifications within a unique framework. Section II outlines the proposed methodology for modifying DMP generated trajectories by pHRI during execution. In section III preliminaries on DMPs are given for point to point movements in the Cartesian space and a novel DMP formulation is presented that enables synchronization with user physical interventions when they occur. Section IV presents a varying stiffness controller that is proved to be passive with respect to the tracking error velocity while all states remain bounded. Experimental results are presented in section V demonstrating the efficacy and performance of the proposed approach.

II. THE PROPOSED pHRI FRAMEWORK

We consider a scenario in which a previously demonstrated point to point trajectory is encoded in a DMP and is used to provide the kinematic reference to the robot during execution. Our objective is to design a method which will enable a user to modify the trajectory at various segments by physical human robot interaction (pHRI) i.e. by directly getting into

[1]Authors are with Aristotle University of Thessaloniki, Department of Electrical and Computer Engineering, Thessaloniki 54124, Greece. e-mail: tkastrit@ece.auth.gr, antosidi@ece.auth.gr, doulgeri@eng.auth.gr

physical contact with the robot during execution and kinesthetically modifying its trajectory. The basic concept of the proposed method involves a robot under varying impedance control that is determined on-line and a DMP structure with user synchronization ability. As long as the robot executes the task by following the DMP produced trajectory without any user interference, its initial stiffness will rise up to a preset level. When the user intervenes, the external force and the tracking error will induce a stiffness decrease and the DMP's time evolution will be synchronized, to facilitate and accommodate any desired trajectory modifications. The synchronization refers to the ability of the proposed DMP to dynamically change its evolution so that its generated position reference is almost the closest point to the current position induced by the user's action, which is not necessarily associated with a small distance. The concept is illustrated in Figure 1 and Figure 2. In figure 1 the one dimensional synchronization is shown depicting the DMP position and velocity trajectories together with an hypothetical user's intervention having a different velocity profile (dashed lines). The synchronized DMP should follow the user's velocity profile rather than generating the originally demonstrated one. In the 2D case, the DMP and the modified path are shown with the synchronized positions along them as time is an implicit parameter. Notice the respective tracking errors being normal to the DMP's path tangent (i.e the DMP's velocity) indicating that the DMP position evolves so that it stays at the nearest distance to the current robot's position.

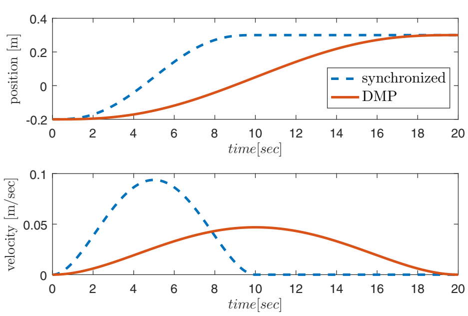

Fig. 1: 1D example of velocity profile synhronization.

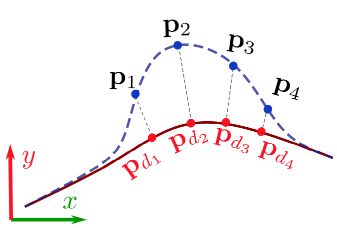

Fig. 2: 2D example with DMP and modnnified path with synchronized DMP evolution.

The proposed method does not involve any switching between the autonomous execution and the user's intervention while it assumes the availability of external force measurement or estimation. Such assumption is not restrictive as it is a feature of currently available collaborative robots via joint torque sensing (e.g. KUKA LWR4+) or via estimation methods (e.g. generalized momentum method [10]). The modified trajectory can serve to retrain the DMP and it will be generated in the next task cycle until the user is satisfied and no further interventions are needed. The variable stiffness is applied via a tank-based approach to preserve the controlled system's passivity with respect to the tracking error velocity while all states remain bounded.

III. DMP Synchronization in pHRI Tasks

A. Preliminaries

In the last decades, there are many works which use programming by demonstration (PbD) to avoid tedious hand programming processes. Human motion capture data or robot kinesthetic teaching is utilized for learning complex kinematic behaviors that are encoded with dynamical systems. In this direction, dynamic movement primitives (DMPs) have been proposed [1] and used to generate both joint [2] and end-effector movements [11]. They consist of two dynamical systems, the transformation system and the canonical system, The former encodes each relevant task coordinate with a compact representation and the latter controls time evolution via a phase variable and is common for all transformation systems. DMP enable incorporation of sensory feedback in either or both systems to allow modifications of the learned trajectory or the phase variable evolution.

A DMP for a point to point movement in the Cartesian space $\mathbf{y} \in \mathbb{R}^3$ is typically defined by the following set of nonlinear system equations:

$$\begin{aligned} \tau\dot{\mathbf{z}} &= a_z(b_z(\mathbf{g}-\mathbf{y})-\mathbf{z})+\mathbf{F}(x) \\ \tau\dot{\mathbf{y}} &= \mathbf{z} \end{aligned} \tag{1}$$

where $\mathbf{g} \in \mathbb{R}^3$ is the desired final position on the movement, $\tau \in \mathbb{R}^+$ is the trajectory's total time that can be used to scale the DMP response temporaly during execution, $a_z, b_z \in \mathbb{R}^+$ are positive gains with the choice of $a_z = 4b_z$ leading to a critically damped linear part of the equation and $\mathbf{F}(x)$ is a combination of nonlinear functions with N Gaussian kernels:

$$\mathbf{F}(x) = diag(\mathbf{g}-\mathbf{y}_0)\frac{\sum_{i=1}^{N}\mathbf{W}^i\psi_i(x)}{\sum_{i=1}^{N}\psi_i(x)}x \tag{2}$$

$$\psi_i(x) = \exp(-h_i(x-c_i)^2) \tag{3}$$

where $\psi_i(x)$ are Gaussian kernels, with c_i being the center of the Gaussian kernel and h_i the inverse width while $\mathbf{W}^i$ are the columns of the weight matrix $\mathbf{W} \in \mathbb{R}^{3\times\mathrm{N}}$ calculated during learning by Locally Weighted Regression (LWR) to encode the desired shape of the demonstrated trajectory. The diagonal matrix $diag(\mathbf{g}-\mathbf{y}_0)$ in (2) is a spatial scaling factor while x is the phase variable utilized to avoid direct dependence on time. A typical choice for the canonical system that yields an exponential response of x from the initial value $x_0 = 1$ to 0 is the following:

$$\tau\dot{x} = -\alpha_x x, \quad x(0) = 1 \tag{4}$$

where $a_x \in \mathbb{R}^+$ is a user defined gain. Notice that $\mathbf{F}(x) \rightarrow 0$ for $t \rightarrow \infty$, since $x \rightarrow 0$ and subsequently system (1) has a unique stable equilibrium at $\mathbf{y} = \mathbf{g}$.

DMP enable incorporation of sensory feedback in either or both systems to allow modifications of the learned trajectory or the phase variable evolution. Let the robot's end-effector position $\mathbf{p}$ be different from the reference position $\mathbf{y}$ generated by the DMP during execution. The existence of the tracking error $\mathbf{p}-\mathbf{y}$ may be attributed to external disturbances and is not unusual during execution. In the presence of such tracking errors the most typical approach to adapt the DMP is known as phase stopping and is achieved by modifying the canonical system as follows [1]:

$$\tau \dot{x} = -\frac{a_x}{1 + n_x||\mathbf{p} - \mathbf{y}||} x$$

where $n_x \in \mathbb{R}^+$ is a prespecified constant gain. If the tracking error $||\mathbf{p}-\mathbf{y}||$ is large, the evolution of the phase variable practically stops yielding an almost constant non-linear term $\mathbf{F}(x)$ in the transformation system (1). Consequently the reference position converges to a steady state value $\mathbf{y}_s$ until the error $||\mathbf{p} - \mathbf{y}_s||$ is reduced again.

B. Synchronizing DMP evolution with user induced velocity

In this work, we want to synchronize the DMP's evolution with the user movement during pHRI by speeding up or slowing down the dynamical system's evolution (1) as appropriate. It is clear that phase stopping does not address this synchronization problem since any speeding up even along the DMP learned path would stop the evolution rather than adapting it to the induced velocity by the user's interaction force. In what follows we propose a DMP structure that decreases the tracking errors produced by the lack of synchronization between the DMP's evolution and the user while interacting with the robot. In order to achieve the synchronization goal in point to point movements, we introduce an extra dynamical system in the original formulation which is responsible for the adaptation of the trajectory's total time or duration (τ in (1), (4)). The proposed duration adaptive law is given by:

$$\dot{\tau} = \begin{cases} a_\tau \left(\dfrac{\tau_s}{\xi + \epsilon} - \tau \right) & \text{if } \xi > 0 \\ a_\tau \left(\dfrac{\tau_s}{\epsilon} - \tau \right) & \text{otherwise} \end{cases}, \tag{5}$$

$$\xi = 1 + n_y(\mathbf{p} - \mathbf{y})^T \dot{\mathbf{y}} \tag{6}$$

where $a_\tau, n_y \in \mathbb{R}^+$ are constant gains, $\tau_s \in \mathbb{R}^+$ is the time duration measured during the demonstration or set for the autonomous operation, $\tau(0) = \tau_s$, and $\epsilon \in \mathbb{R}^+$ is a small constant ($\ll 10^{-3}$) needed to avoid possible singularities. Notice that the system (5), (6) is differentiable and that if $||\mathbf{p} - \mathbf{y}|| = 0$, $\xi = 1$ in which case $\tau \rightarrow \tau_s$ as $t \rightarrow \infty$ and $\epsilon \rightarrow 0$. Further notice that the second term of ξ may take negative values when the user is slower than the DMP triggering the second case of (5) and thus literally slowing down the DMP evolution. If the user is faster than the DMP evolution, the second term of ξ is positive, hence $\xi > 1$, literally speeding up the DMP evolution.

IV. A PASSIVE VARYING STIFFNESS CONTROLLER

Within the scope of this paper we consider only robot end-effector positions. Hence, we consider the case of a 3-dof non-redundant manipulator. The robot's dynamic model compensated for gravity can be written in Cartesian space as follows:

$$\mathbf{\Lambda}_p(\mathbf{q})\ddot{\mathbf{p}} + \mathbf{C}_p(\mathbf{q}, \dot{\mathbf{q}})\dot{\mathbf{p}} = \mathbf{F}_p + \mathbf{F}_c \tag{7}$$

where

$$\mathbf{\Lambda}_p(\mathbf{q}) = [\mathbf{J}(\mathbf{q})\mathbf{\Lambda}(\mathbf{q})^{-1}\mathbf{J}(\mathbf{q})^T]^{-1} \tag{8}$$

$$\mathbf{C}_p(\mathbf{q}, \dot{\mathbf{q}}) = \mathbf{J}(\mathbf{q})^{-T}\mathbf{C}(\mathbf{q}, \dot{\mathbf{q}})\mathbf{q} - \mathbf{\Lambda}_x(\mathbf{q})\dot{\mathbf{J}}(\mathbf{q})\dot{\mathbf{q}} \tag{9}$$

with $\mathbf{q} \in \mathbb{R}^3$ being the joint positions, $\mathbf{J}(\mathbf{q}) \in \mathbb{R}^{3\times3}$ the robot's Jacobian, $\mathbf{\Lambda}(\mathbf{q}) \in \mathbb{R}^{3\times3}$ the manipulator's inertia matrix, $\mathbf{C}(\mathbf{q}, \dot{\mathbf{q}}) \in \mathbb{R}^{3\times3}$ the Coriolis and centripetal matrix, $\mathbf{p} \in \mathbb{R}^3$ the current end effector position, $\mathbf{F}_p \in \mathbb{R}^3$ the external force applied to the end-effector and $\mathbf{F}_c \in \mathbb{R}^3$ is a control signal. Notice that the task space inertia matrix $\mathbf{\Lambda}_p$ is positive define and the matrix $\dot{\mathbf{\Lambda}}_p - 2\mathbf{C}_p$ is skew symmetric.

Let a desired position trajectory be denoted by $\mathbf{p}_d$, $\dot{\mathbf{p}}_d$ $\ddot{\mathbf{p}}_d$ which, in this work, is provided by the proposed DMP structure. In order to achieve a target Cartesian impedance we utilize the following model based control signal that imposes a desired Cartesian stiffness and damping without shaping the inertia:

$$\mathbf{F}_c = \mathbf{\Lambda}_p(\mathbf{q})\ddot{\mathbf{p}}_d - \mathbf{D}_d\dot{\tilde{\mathbf{p}}} - \mathbf{K}_c\tilde{\mathbf{p}} + \mathbf{C}_p(\mathbf{q}, \dot{\mathbf{q}})\dot{\mathbf{p}}_d + \mathbf{u}_c \tag{10}$$

where $\tilde{\mathbf{p}} := \mathbf{p} - \mathbf{p}_d(t) \in \mathbb{R}^3$ is the tracking error, $\mathbf{K}_c = k_c\mathbf{I}_{3\times3} \in \mathbb{R}^{3\times3}$, $\mathbf{D}_d \in \mathbb{R}^{3\times3}$ are positive definite matrices of the desired stiffness and damping respectively and $\mathbf{u}_c \in \mathbb{R}^3$ is an extra control input to be defined later. In case joint velocity measurements are not available, they can be estimated by numerically differentiating joints position measurements. In case of kinesthetic guidance, motion is relatively slow, making this estimation valid. Alternatively, a linear velocity observer [12] can be utilized.

Substituting $\mathbf{F}_c$ from (10) in (7) yields the following non-linear closed loop system:

$$\mathbf{\Lambda}_p(\mathbf{q})\ddot{\tilde{\mathbf{p}}} + (\mathbf{C}_p(\mathbf{q}, \dot{\mathbf{q}}) + \mathbf{D}_d)\dot{\tilde{\mathbf{p}}} + \mathbf{K}_c\tilde{\mathbf{p}} = \mathbf{F}_p + \mathbf{u}_c \tag{11}$$

It is known that in the absence of any input ($\mathbf{F}_p = \mathbf{0}, \mathbf{u}_c = \mathbf{0}$) the equilibrium state of (11) is globally asymptotically stable yielding the desired trajectory tracking [13]. It is further easy to prove utilizing the storage function $V_s = \dfrac{\dot{\tilde{\mathbf{p}}}^T\mathbf{\Lambda}_p(\mathbf{q})\dot{\tilde{\mathbf{p}}}}{2} + \dfrac{\tilde{\mathbf{p}}^T\mathbf{K}_c\tilde{\mathbf{p}}}{2}$ that the system (11) represents a passive mapping from a disturbance input to the velocity tracking error $\dot{\tilde{\mathbf{p}}}$. Notice that in the presence of a disturbance input induced by model uncertainties and/or unmodeled dynamics (e.g. friction, backlash), the norm of the tracking error depends on the stiffness value. The higher is the desired stiffness the smaller is the tracking error achieved.

To serve the objective of kinesthetically modifying the executed trajectory during the robot's autonomous motion it is important to introduce a varying stiffness that would facilitate the user in his task. To this aim we augment the desired stiffness by adding a varying stiffness matrix $\mathbf{K}_v(t)$ initially proposed in [3]. In particular,

$$\mathbf{K}_v = k(t)\mathbf{I}_{3\times 3} \tag{12}$$

updated at each control cycle by the following rate law:

$$\dot{k}(t) = \begin{cases} max(w,0) & k(t)=0 \\ w & 0<k(t)<k_{max} \\ min(w,0) & k(t)=k_{max} \end{cases} \tag{13}$$

where

$$w = k_f f(k)\left(1 - \frac{k}{k_c}\frac{||\mathbf{F}_p||}{\lambda_2} - \frac{||\tilde{\mathbf{p}}||}{\lambda_1}\right) \tag{14}$$

$$f(k) = \sqrt{k} + w_{min} \tag{15}$$

with k_{max} being a preset constant value representing the maximum added value to the stiffness yielding a maximum desired stiffness of $\mathbf{K}_c + k_{max}\mathbf{I}$, k_f is a gain applied to the stiffness rate, λ_1, λ_2 are user defined thresholds for the tracking error $\tilde{\mathbf{p}}$ and the external force $||\mathbf{F}_p||$ respectively and w_{min} is set to reflect the minimum rate of stiffness increase in the absence of errors and external forces when $k=0$. The value of $k(0)$ and of the parameter λ_1 is selected so that the small tracking errors that may exist owing to modeling errors will not prevent the stiffness from rising in the absence of an external force. The form of (14) ensures that the stiffness will decrease rapidly in the presents of the applying external force and tracking error and its rate will be magnified the higher is the stiffness at the moment of interaction.

The introduction of a variable stiffness $\mathbf{K}_v$ in the system (11) may leads to loss of passivity [14]. This problem can be resolved by applying the varying stiffness via a tank energy based approach proposed in [8], which has shown to preserve passivity in other cases [15]. The main idea is to endow the variable stiffness with an energy tank variable storing the energy dissipated by the system and reusing it when needed. In particular, the variable stiffness is applied by the following extra control input:

$$\mathbf{u}_c = -\beta(p_t)\mathbf{K}_v\tilde{\mathbf{p}} \tag{16}$$

where p_t is an additional virtual state variable that represents the stored energy and which is given by the following dynamic equation:

$$\dot{p}_t = \frac{\mu(p_t)}{2}\dot{\tilde{\mathbf{p}}}^T\mathbf{D}_d\dot{\tilde{\mathbf{p}}} + \beta(p_t)\tilde{\mathbf{p}}^T K_v\dot{\tilde{\mathbf{p}}} \tag{17}$$

where $\mu(p_t), \beta(p_t)$ are scalar functions which control the flow of energy between the virtual storage p_t and the robot. The virtual state p_t must only store a finite amount of energy which is expressed by the upper limit $\overline{p_t} > 0$. The scalar functions $\mu(p_t), \beta(p_t)$ are defined as follows:

$$\mu(p_t) = \begin{cases} 1, & \text{if } p_t \le \overline{p_t} \\ 0, & \text{otherwise} \end{cases} \tag{18}$$

$$\beta(p_t) = \begin{cases} 0, & \text{if } (p_t \ge \overline{p_t} \wedge \tilde{\mathbf{p}}^T K_v\dot{\tilde{\mathbf{p}}} > 0) \\ & \vee(p_t = 0 \wedge \tilde{\mathbf{p}}^T K_v\dot{\tilde{\mathbf{p}}} < 0) \\ 1, & \text{otherwise} \end{cases} \tag{19}$$

Remark 1: To avoid the sharp changes in control, $\mu(p_t)$ and $\beta(p_t)$ can be defined as smooth transition functions between 0 to 1. For $\beta(p_t)$ a combination of smooth functions of p_t and $\tilde{\mathbf{p}}^T K_v\dot{\tilde{\mathbf{p}}}$ can be utilized, as it can be found for example in [15].

Notice that by selecting $0 \le p_t(0) \le \overline{p_t}$ and owing to (17), (18) and (19), $p_t \in \Omega,\ \forall t > 0$ with $\Omega \in \{p_t \in \mathbb{R} : 0 \le p_t \le \overline{p_t}\}$. Substituting (16) in (11) we get the following dynamics:

$$\mathbf{\Lambda}_p(\mathbf{q})\ddot{\tilde{\mathbf{p}}} + (\mathbf{C}_p(\mathbf{q},\dot{\mathbf{q}}) + \mathbf{D}_d)\dot{\tilde{\mathbf{p}}} + (\mathbf{K}_c + \beta(p_t)\mathbf{K}_v)\tilde{\mathbf{p}} = \mathbf{F}_p \tag{20}$$

Define now the state vector $\mathbf{s} = [\dot{\tilde{\mathbf{p}}}^T\ \tilde{\mathbf{p}}^T\ p_t]^T \in (\mathbb{R}^3 \times \mathbb{R}^3 \times \Omega)$ and the input $\mathbf{F}_p$. The closed-loop system (20), (17) can be written in the following compact form:

$$\dot{\mathbf{s}} = \mathbf{H}(\mathbf{s},\mathbf{F}_p),\ \mathbf{s}_0 = \mathbf{s}(0) \in D \tag{21}$$

where $D = \{\mathbf{s} : \mathbf{s} \in \mathbb{R}^3 \times \mathbb{R}^3 \times \Omega\}$ and

$$\mathbf{H}(\mathbf{s},\mathbf{F}_p) = \begin{bmatrix} \mathbf{\Lambda}_p^{-1}(-(\mathbf{C}_p + \mathbf{D}_d)\dot{\tilde{\mathbf{p}}} - \mathbf{K}_c\tilde{\mathbf{p}} + \mathbf{F}_p + \mathbf{u}_c) \\ \dot{\tilde{\mathbf{p}}} \\ \frac{\mu(p_t)}{2}\dot{\tilde{\mathbf{p}}}^T\mathbf{D}_d\dot{\tilde{\mathbf{p}}} + \beta(p_t)\tilde{\mathbf{p}}^T\mathbf{K}_v\dot{\tilde{\mathbf{p}}} \end{bmatrix}.$$

Theorem 1: The following statements are valid:

(1) The system dynamics (21) represents a passive mapping from the external human force $\mathbf{F}_p$ to the velocity $\dot{\tilde{\mathbf{p}}}$,

(2) The state of the system (21) is bounded under the exertion of human force $\mathbf{F}_p$.

Proof: 1) Consider the positive storage function :

$$V = \frac{\dot{\tilde{\mathbf{p}}}^T\mathbf{\Lambda}_p\dot{\tilde{\mathbf{p}}}}{2} + \frac{\tilde{\mathbf{p}}^T\mathbf{K}_c\tilde{\mathbf{p}}}{2} + p_t \tag{22}$$

Taking the time derivative of (22) yields

$$\dot{V} = \frac{1}{2}\dot{\tilde{\mathbf{p}}}^T\dot{\mathbf{\Lambda}}_p\dot{\tilde{\mathbf{p}}} + \dot{\tilde{\mathbf{p}}}^T\mathbf{\Lambda}_p\ddot{\tilde{\mathbf{p}}} + \tilde{\mathbf{p}}^T\mathbf{K}_c\dot{\tilde{\mathbf{p}}} + \dot{p}_t \tag{23}$$

Substituting $\mathbf{\Lambda}_p\ddot{\mathbf{p}}$ from (20) in (23), and utilizing the skew-symmetry of matrix $\left(\dot{\mathbf{\Lambda}}_p - 2\mathbf{C}_p\right)$, yields:

$$\dot{V} = -\dot{\tilde{\mathbf{p}}}^T\mathbf{D}_d\dot{\tilde{\mathbf{p}}} + \mathbf{F}_p^T\dot{\tilde{\mathbf{p}}} - \beta(p_t)\tilde{\mathbf{p}}^T\mathbf{K}_v\dot{\tilde{\mathbf{p}}} + \dot{p}_t \tag{24}$$

Substituting $\dot{p}_t$ from (17), $\dot{V}$ becomes:

$$\dot{V} = -(1 - \frac{\mu(p_t)}{2})\dot{\tilde{\mathbf{p}}}^T\mathbf{D}_d\dot{\tilde{\mathbf{p}}} + \mathbf{F}_p^T\dot{\tilde{\mathbf{p}}} \tag{25}$$

Since $\mu(p_t) \in \{0,1\}$

$$\dot{V} \le -\frac{1}{2}\dot{\tilde{\mathbf{p}}}^T\mathbf{D}_d\dot{\tilde{\mathbf{p}}} + \mathbf{F}_p^T\dot{\tilde{\mathbf{p}}} \tag{26}$$

yielding the strict passivity of the pair $\mathbf{F}_p$, $\dot{\tilde{\mathbf{p}}}$ for (21).

2) To prove the second part of theorem, notice that (26) can be further manipulated by completing the squares as follows:

$$\begin{aligned} \dot{V} &= -||\sqrt{\frac{\mathbf{D}_d}{2}}\dot{\tilde{\mathbf{p}}} - \sqrt{2\mathbf{D}_d}^{-1}\mathbf{F}_p||^2 + \frac{1}{2}\mathbf{F}_p^T\mathbf{D}_d^{-1}\mathbf{F}_p \\ &\le \frac{1}{2}\mathbf{F}_p^T\mathbf{D}_d^{-1}\mathbf{F}_p. \end{aligned} \tag{27}$$

Notice that $\mathbf{F}_p$ represents the force applied by the human to guide the robot. Thus, $\mathbf{F}_p$ is bounded, therefore $\mathbf{F}_p^T \mathbf{D}_d^{-1} \mathbf{F}_p$ is bounded and since the human forces have bounded energy, taking the integral of equation (27), yields:

$$V \leq V(t_0) + \int_{t_0}^{t} \frac{1}{2} \mathbf{F}_p^T \mathbf{D}_d{}^{-1} \mathbf{F}_p \partial\tau < \infty \tag{28}$$

which implies boundedness of state $p_t, \dot{\tilde{\mathbf{p}}}$ and $\tilde{\mathbf{p}}$. ■

V. EXPERIMENTAL RESULTS

To demonstrate the effectiveness of the proposed methodology, a 7-dof KUKA LWR4+ robotic manipulator was utilized under Cartesian impedance control locking the end-effector's orientation. The proposed methodology was implemented in C++ utilizing the FRI library with control frequency $\mathrm{f_s} = 1000$ Hz. The impedance controller (20) is implemented without feeding forward the desired velocity and acceleration via the inertia and Coriolis/Centrifugal matrices in (11); the assumption is that respective forces are negligible for the tested velocities and accelerations as compared to the rest of the terms.

The user initially moves the end-effector of the gravity compensated robot from a predefined starting position to a predefined target in a time duration of $\tau_s = 13.7sec$. When at target, the proposed DMP with parameter values given in TABLE I is trained producing the required weight values that will allow the DMP to generate the demonstrated trajectory. Then the robot autonomously executes the demonstrated motion using the proposed control law with parameter values also given in TABLE I, while $p_t(0) = 0.04, \overline{p_t} = 10$ and $k(0) = 1000$ are utilized. The value of a_τ is selected to reflect a fast response for τ while the value of a_x ensures that the phase variable is close to zero at τ sec.

TABLE I: Parameter Values

DMP Parameter	Values	Control Parameter	Values
a_z	20	$\mathbf{D}_d$	25 $\mathbf{I}_{3\times3}$
b_z	5	k_c	10
a_τ	800	w_{min}	5
a_x	3	λ_1	0.1
n_y	10^5	λ_2	70
N	110	k_{max}	2000
ϵ	10^{-6}	k_f	12

Experimental results without and with user intervention are depicted in Fig. 3-9. Fig. 3 show that in the lack of an external force and despite control simplifications which result in modeling errors, the tracking error is in the region of one mm. Notice how the varying stiffness $k(t)$, is increased from its initial value to its preset maximum ($k_{max} = 2000$) after 2 sec (a tunable rate of increase) while the total motion duration remains constant at the demonstrated value of $\tau_s = 13.7sec$ (Fig. 4(b)). The exponential phase time evolution is depicted in Fig. 4(a). These results demonstrate a behavior similar to what we would get with the typical DMP structure. Fig. 5 shows the demonstrated path p_{ref} and the generated path by the DMP p_d together with the modified path when the user intervenes to repair the trajectory. In the latter case,

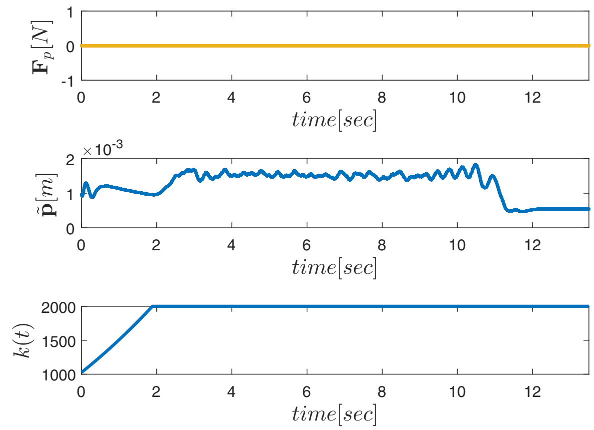

Fig. 3: Experimental results without pHRI.

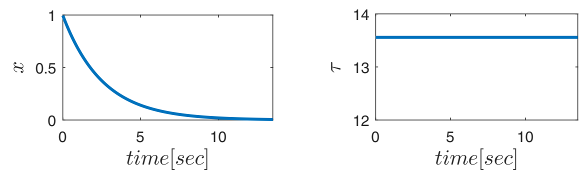

(a) Phase variable (b) Trajectory total time

Fig. 4: DMP phase and duration response without pHRI.

the stiffness and the tracking error response shown in Fig. 6 indicate how the variable stiffness $k(t)$ decreases rapidly while the tracking error is allowed to increase. When the user returns close to the synchronized trajectory he may withdraw; as the tracking error and the force become small in this case $k(t)$ increases again. Control effort is depicted in Fig. 7. The response of the phase variable and the time duration is shown in Fig. 8. Notice how in the time interval $[t_c,\ 5]$ the trajectory's duration obtains a very large value extending beyond the figure range (Fig. 8(b)); as a consequence the phase variable's evolution stopped (Fig. 8(a)). In this small interval the human applies a force to modify the trajectory momentarily stopping the motion hence τ increases. In the next time interval $[5,\ 10]$ when the stiffness has dropped and modifications are realized with little effort, we observe the τ evolution yielding a synchronized DMP. Notice that the total duration of the modified trajectory is now 15.8 sec. Last, the virtual tank energy p_t is depicted in Fig. 9 storing energy when the tracking error increases and dissipating energy when it decreases.

VI. CONCLUSIONS

In this work a control framework is proposed combining an impedance controller with variable stiffness applied via a tank energy approach and a novel DMP motion generator for the robot's tip position that allows synchronization with the intervening user. Output passivity with respect to the human force as well as state boundedness is shown. Experiments demonstrate the efficacy of the approach uni-

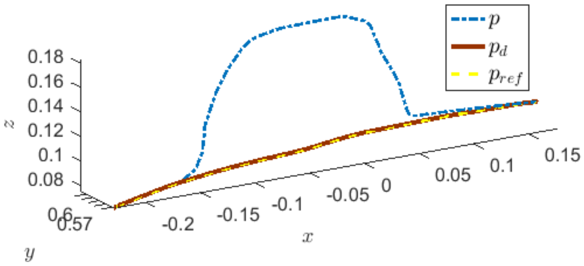

Fig. 5: Experimental results with and without pHRI.

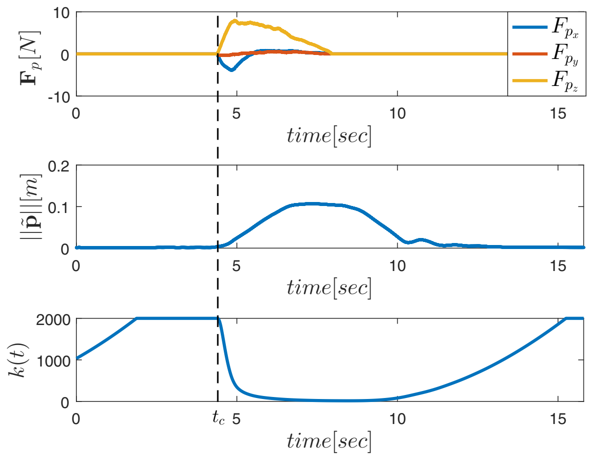

Fig. 6: External force, tracking error and variable stiffness.

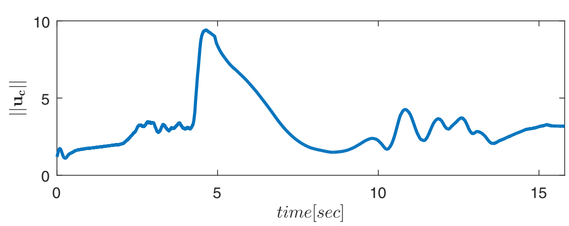

Fig. 7: The norm of the control input $\mathbf{u}_c$.

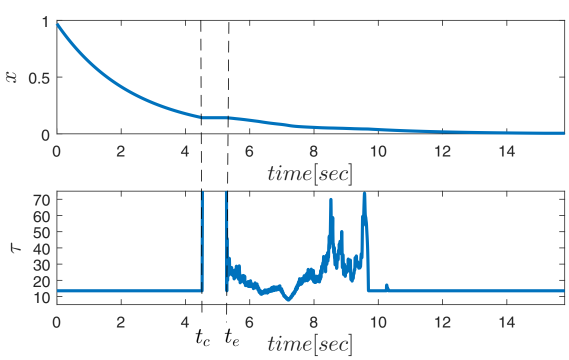

Fig. 8: Response of phase variable and duration with pHRI.

fying autonomous operation and user driven modifications of learned kinematic behaviors. Future work will extend the

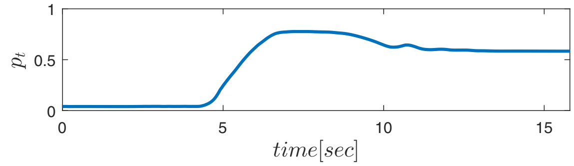

Fig. 9: Tank energy.

proposed method to motions incorporating both position and orientation.

References

[1] S. Schaal, P. Mohajerian, and A. Ijspeert, "Dynamics systems vs. optimal controla unifying view," *Progress in brain research*, vol. 165, pp. 425–445, 2007.

[2] S. Bitzer and S. Vijayakumar, "Latent spaces for dynamic movement primitives," in *Humanoid Robots, 2009. Humanoids 2009. 9th IEEE-RAS International Conference on*. IEEE, 2009, pp. 574–581.

[3] F. Dimeas, F. Fotiadis, D. Papageorgiou, A. Sidiropoulos, and Z. Doulgeri, "Towards progressive automation of repetitive tasks through physical human-robot interaction," in *to appear in Human-Friendly Robotics Workshop, Springer Proceedings in Advanced Robotics*, 2017.

[4] J. Nakanishi, J. Morimoto, G. Endo, G. Cheng, S. Schaal, and M. Kawato, "Learning from demonstration and adaptation of biped locomotion," *Robotics and autonomous systems*, vol. 47, no. 2-3, pp. 79–91, 2004.

[5] F. Ficuciello, L. Villani, and B. Siciliano, "Variable impedance control of redundant manipulators for intuitive human–robot physical interaction," *IEEE Transactions on Robotics*, vol. 31, no. 4, pp. 850–863, 2015.

[6] A. Lecours, B. Mayer-St-Onge, and C. Gosselin, "Variable admittance control of a four-degree-of-freedom intelligent assist device," in *Robotics and Automation (ICRA), 2012 IEEE International Conference on*. IEEE, 2012, pp. 3903–3908.

[7] V. Duchaine and C. M. Gosselin, "General model of human-robot cooperation using a novel velocity based variable impedance control," in *EuroHaptics Conference, 2007 and Symposium on Haptic Interfaces for Virtual Environment and Teleoperator Systems. World Haptics 2007. Second Joint*. IEEE, 2007, pp. 446–451.

[8] F. Ferraguti, C. Secchi, and C. Fantuzzi, "A tank-based approach to impedance control with variable stiffness," in *Robotics and Automation (ICRA), 2013 IEEE International Conference on*. IEEE, 2013, pp. 4948–4953.

[9] V. Duindam and S. Stramigioli, "Port-based asymptotic curve tracking for mechanical systems," *European Journal of Control*, vol. 10, no. 5, pp. 411–420, 2004.

[10] A. De Luca, A. Albu-Schaffer, S. Haddadin, and G. Hirzinger, "Collision detection and safe reaction with the dlr-iii lightweight manipulator arm," in *Intelligent Robots and Systems, 2006 IEEE/RSJ International Conference on*. IEEE, 2006, pp. 1623–1630.

[11] P. Hung and T. Yoshimi, "An approach to learn hand movements for robot actions from human demonstrations," in *System Integration (SII), 2016 IEEE/SICE International Symposium on*. IEEE, 2016, pp. 711–716.

[12] S. Arimoto, "A class of linear velocity observers for nonlinear mechanical systems," in *Proc. of 1st Asian Control Conference*, vol. 2, 1994, pp. 633–636.

[13] C. Ott, "Cartesian impedance control: The rigid body case," in *Cartesian Impedance Control of Redundant and Flexible-Joint Robots*. Springer, 2008, pp. 29–44.

[14] K. Kronander and A. Billard, "Stability considerations for variable impedance control," *IEEE Transactions on Robotics*, vol. 32, no. 5, pp. 1298–1305, 2016.

[15] ——, "Passive interaction control with dynamical systems," *IEEE Robotics and Automation Letters*, vol. 1, no. 1, pp. 106–113, 2016.